Statistical Analysis of Low Frequency Responses of a Moored Floating Offshore Structure (1st Report)*

By

Shunji KATO** and Sadao ANDO**

ABSTRACTS

The purpose of this paper is to estimate the response statistics of a moored floating structure that can be modelled as the two term Volterra series expansion subjected to a stationary Gaussian random waves.

For estimating the instantaneous probability density function of response the approximate method using the finite Gram-Charlier expansion and the asymptotic form of the exact solution which can be obtained from Kac-Siegert method is proposed. In order to estimate the probability density function of extremal values consisting maxima and minima and the extreme responses the assumptions in which response and response velocity are mutually independent and the velocity is a Gaussian process with zero mean are introduced in addition to Powell's assumptions in the field of structural dynamics.

The frequency properties have been found experimentally through cross spectral and cross bispectral analyses.

Comparisons between the experimental results and the statistical ones estimated from the frequency properties of response are discussed. As the results it has been confirmed that both results show a fairly good agreement.

1. INTRODUCTION

For a moored floating structure if the static restoring force by mooring lines is very small, it is possible that a highly tuned resonance generally occurs at very low natural frequencies in horizontal plane. In irregular waves this resonance will be excited by the slowly varying second order wave excitation which corresponds to the drifting force in regular waves. Thus, for the design of mooring lines it is necessary to include these forces in the total load acting on a structure moored by chains or cables.

Up to now, several investigations associated with these second order responses (forces or motions) have been done.

These studies can be classified as follows :

1) Deterministic manner based on the numerical simulations.

2) Nondeterministic manner based on the stochastic process.

The former is the numerical prediction method based on the solution of the

* Received on May 6, 1986

** Ocean Engineering Division

time dependent motion equation taking into account of both the first order forces due to wave elevation and the second order forces which are obtained from the direct integration of all second order pressures over the instantaneous wetted portions of the hull surface. But since the nonlinear second order response depends on the random phases of waves the results derived by this manner are nothing but one sample.

Therefore, in order to estimate the extreme value by means of this manner numerous results of numerical simulations are required.

The latter is the statistical prediction method based on the Volterra functional series expansion of responses to the given wave or force excitation. The advantage of this method is that it is easily adaptable to the physical interpretation associated with the usual perturbation expansion solution of nonlinear response problems because the n-th term in such a expansion gives the response component resulting form n-th order interaction of the excitation.

Hasselmann[1] outlined the functional series approach to ship motions and showed that the nonlinear transfer functions were related to higher-order moments of ship motions. Dalzel[2] formulated the added resistance in waves as the quadratic functional series and estimated the mean added resistance transfer function in irregular waves.

Neal[3] formulated the exact probability density function of second order responses by using the statistical theory of quadratic form.

Vinje[4] obtained the approximate expressions of peak distributions of second order responses by use of the expansion of cumulants. Further he[5] expanded Neal's formulation to peak distribution under Powell's assumptions. Hineno[6] applied Vinje's method to the nonlinear wave and the steady tilt problem for a semisubmersible drilling platform.

The present authors et al.[7] showed that the probability densities of mooring forces on the huge offshore structure can be represented by the finite Gram-Charlier expansion.

Recently, Naess[8] discussed the dynamic reliability of second order responses under the Poisson distribution by means of Neal's formulation and the slow drift approximation.

The authors[9] have already shown that the Kac-Siegert method adopted in Neal's work is applicable to the horizontal responses of a moored floating structure and the quadratic transfer function treated in Dalzel's work is required to estimate the higher-order statistical values (variance, skewness and etc.) .

As described in the above overview the statistical theory on second order responses is nearly completed. But the discussions for the extreme responses and the approximate theory have not been done sufficiently.

The purpose of this paper is to discuss the extreme values and the approximate statistical theory for the horizontal responses of a moored floating structure.

In chapter 2 the Kac-Siegert theory[10),11)] on second order responses is discussed in details.

In chapter 3 the approximate theory and the estimation method of extreme value in case of the horizontal responses are developed.

In chapter 4 the applicability of the methods introduced in chapter 3 is investigated through the comparisons between the experimental results and the estimated values.

As the results the following items have been found:

(1) The transfer function of the horizontal response to the slowly instantaneous wave energy, which is introduced newly in this case, is able to evaluate quantitatively the characteristics of the quadratic transfer function, and the linear transfer function can be separated from the total response in the frequency domain and can be estimated by the usual linear motion prediction method taking the viscous damping into account.

By using these functions the variance and the skewness which dominate the distribution of the horizontal response can be estimated.

(2) In order to obtain the instantaneous probability distribution we propose the approximate method matching between the finite Gram-Charlier expansion and the asymptotic form derived from the Kac-Siegert theory. The estimated results due to the present method show fairly good agreement with the experimental ones.

(3) The new prediction methods for the probability distributions of extremal values and the extreme response are proposed under the assumptions that the response displacement and velocity are independent mutually and the response velocity is of Gaussian distribution with zero mean in addition to the Powell's assumptions. As a result it is confirmed that the Longuet-Higgin's method significantly underestimates the experimental result while the present method is in good agreement with the experimental one.

2. EXACT STATISTICAL THEORY

2.1 Basic Assumptions

The assumption of this theory is that the nonlinear responses can be represented by the functional power series (or functional polynomials).

Let $x(t)$ denote the nonlinear response of a moored floating structure to a random excitation $\{\zeta(t) \mid t \in R^1\}$. Since $x(t)$ may be the responses to the entire time history of $\zeta(t)$, we call $x(t)$ a functional defined on a class of excitation functions $\zeta(t)$ as

$$x(t)=\boldsymbol{F}\,[\xi(t)] \tag{2.1.1}$$

If $\boldsymbol{F}$ is a continuous functional of $\xi(t)$ in the function space sense, then $\boldsymbol{F}$ can be expanded in a functional power series such that

$$x(t)=\sum_{n=0}^{\infty}\int\cdots\int \tilde{g}_n\,(t,\ t_1,\ \cdots\cdots,\ t_n)\,\xi(t_1)\cdots\cdots\xi(t_n)\,dt_1\cdots\cdots dt_n. \tag{2.1.2}$$

If this series represents a causal physical system, then the kernel functions satisfy

$$\tilde{g}_n\,(t,\ t_1,\ \cdots\cdots,\ t_n)=0\,,\ \textit{for}\ t_i>t. \tag{2.1.3}$$

Series satisfying this property were studied by Volterra[12], and series of the form (2.1.2) that satisfy Eq. (2.1.3) are called Volterra series.

If the nonlinear system is time invariant, then kernel functions in Eq. (2.1.2) depend only on time difference. Thus,

$$x(t)=\sum_{n=1}^{\infty}\int_{\tau_1}\!\!d\tau_1\cdots\cdots\int_{\tau_n}\!\!d\tau_n g_n(\tau_1,\ \cdots\cdots,\ \tau_n)\prod_{r=1}^{n}\xi(t-\tau_r)+\text{D. C.}, \tag{2.1.4}$$

where D. C. is a constant.

In general, the kernel functions in Eq. (2.1.4) may not be symmetric functions of their arguments. However, a permutation of indices in any kernel only affects the order in which the integration is carried out but does not affect the response. Thus, for the purpose of analysis, symmetric kernel may be assumed without loss of generality.

If the kernels are continuous and absolutely integrable and if the input is bounded and the contribution from terms of order n in Eq. (2.1.4) decreases to zero as $n\to\infty$, then it is proved that the functional power series (2.1.4) converge uniformly.

We shall limit our analysis to include excitation effects through second order except for D. C.. Thus Eq. (2.1.4) is truncated at $n=2$ and takes the following form:

$$x(t)=\int_{\tau}d\tau g_1(\tau)\,\xi(t-\tau)+\int_{\tau_1}d\tau_1\int_{\tau_2}d\tau_2 g_2(\tau_1,\ \tau_2)\,\xi(t-\tau_1)\,\xi(t-\tau_2) \tag{2.1.5}$$

If $\xi(t)$ is the wave excitation, this series can be used to analyze the response that is proportional to either the wave height or the squared wave height.

If the kernels in Eq. (2.1.5) are continuous and absolutely integrable, then they possess Fourier transform. The transform pairs are defined as follows:

$$\begin{aligned} g_1(\tau)&=1/2\pi\int_{\omega}\exp(i\omega\tau)\,G_1(\omega)\,d\omega,\\ G_1(\omega)&=\int_{\tau}\exp(-i\omega\tau)\,g_1(\tau)\,d\tau, \end{aligned} \tag{2.1.6}$$

$$g_2(\tau_1,\ \tau_2)=1/(2\pi)^2\int_{\omega_1}\!\!d\omega_1\int_{\omega_2}\!\!d\omega_2\exp\{i(\omega_1\tau_1+\omega_2\tau_2)\}\,G_2\ (\omega_1,\ \omega_2),$$

$$G_2(\omega_1, \omega_2) = \int_{\tau_1} d\tau_1 \int_{\tau_2} d\tau_2 \exp\{-i(\omega_1\tau_1 + \omega_2\tau_2)\} g_2(\tau_1, \tau_2).$$

In Eq. (2.1.5) the kernel g_1 is a linear impulse response function, and its transform, G_1, is a linear transfer function. The kernel g_2 is analogous to the linear impulse response function and is called "quadratic impulse response function". Its transform, G_2, is called "quadratic transfer function". Tick[13] has called Eq. (2.1.5) as a time-invariant quadratic system since it includes both a first order and a second order term.

Since the kernel $g_2(\tau_1, \tau_2)$ can be assumed to be symmetrical in its arguments

$$g_2(\tau_1, \tau_2) = g_2(\tau_2, \tau_1), \tag{2.1.7}$$

thus

$$G_2(\omega_1, \omega_2) = G_2(\omega_2, \omega_1). \tag{2.1.8}$$

Consequently, the quadratic transfer function is symmetrical about the line $\omega_1 = \omega_2$ in the (ω_1, ω_2) plane.

2.2 Transfer Functions and their Physical Properties

It is assumed that the surface elevation $\zeta(t)$ is a stationary Gaussian process with zero mean. The auto-correlation function of the process will be denoted as $R_\zeta(t)$ and is defined as follows:

$$R_\zeta(\tau) = E\{\zeta(t)\zeta(t+\tau)\}, \tag{2.2.1}$$

where $E\{\ \}$ denotes the ensemble average (or expectation).

If $R_\zeta(\tau)$ is absolutely integrable, then a continuous nonnegative spectral density function $S_\zeta(\omega)$ exists and satisfies

$$R_\zeta(\tau) = \int_\omega \exp(i\omega\tau) S_\zeta(\omega)\, d\omega, \tag{2.2.2}$$

$$S_\zeta(\omega) = 1/2\pi \int_\tau \exp(-i\omega\tau) R_\zeta(\tau)\, d\tau, \tag{2.2.3}$$

where S_ζ is the two sided wave spectral density function defined over doubly infinities. They are called the Wiener-Khintchine relations.

Taking the expected value of Eq. (2.1.5) we have

$$E\{x\} = \bar{x} = \int_{\tau_1} d\tau_1 \int_{\tau_2} d\tau_2 g_2(\tau_1, \tau_2) R_\zeta(\tau_1 - \tau_2). \tag{2.2.4}$$

Applying Parseval's formula and using the Dirac delta function $\delta(\omega)$, then Eq. (2.2.4) can be written as:

$$\begin{aligned} E\{x\} &= \int_{-\infty}^{\infty} d\omega G_2(\omega, -\omega) S_\zeta(\omega) \\ &= \int_0^{\infty} d\omega G_2(\omega, -\omega) U_\zeta(\omega), \end{aligned} \tag{2.2.5}$$

where U_ζ is the one sided wave spectral density function defined over non-negative frequencies by

$$U_\xi(\omega)=\begin{cases} 2\ S_\xi(\omega) & for\ 0\leqq\omega<\infty \\ 0 & otherwise. \end{cases} \tag{2.2.6}$$

Pinkster[14] has shown that the time average $\bar{x}$ in Eq. (2.1.5) represents the mean drift displacement due to the steady force.

According to his results, the following relation is satisfied:

$$\bar{x}=2\int_0^\infty d\omega H_L(\omega)F_D(\omega)U_\xi(\omega), \tag{2.2.7}$$

where H_L is the linear transfer fuction of displacement to the external force and F_D is the drift force coefficient in regular waves.

Equating Eq. (2.2.5) and Eq. (2.2.7) the following relation

$$G_2(\omega,-\omega)=2H_L(\omega)F_D(\omega) \tag{2.2.8}$$

is found out. Thus, it is found that $G_2(\omega,-\omega)$ represents the mean drift displacement.

Using the fact that $\xi(t)$ is a Gaussian process with zero mean, the second term in eq. (2.1.5) becomes

$$\begin{aligned}&\int_{\tau_1}d\tau_1\int_{\tau_2}d\tau_2 g_2(\tau_1,\tau_2)\xi(t-\tau_1)\xi(t-\tau_2)\\&\quad=1/2R_e\int_0^\infty\int_0^\infty G_2(\omega_1,\omega_2)\exp\{i(\omega_1+\omega_2)t-i(\varepsilon_1+\varepsilon_2)\}\\&\quad\times\sqrt{2U_\xi(\omega_1)2U_\xi(\omega_2)d\omega_1 d\omega_2}\\&\quad+1/2R_e\int_0^\infty\int_0^\infty G_2(\omega_1,-\omega_2)\exp\{i(\omega_1-\omega_2)t-i(\varepsilon_1-\varepsilon_2)\}\\&\quad\times\sqrt{2U_\xi(\omega_1)2U_\xi(\omega_2)d\omega_1 d\omega_2},\end{aligned} \tag{2.2.9}$$

where ε_i are the random phases and statistically independent.

The first term in (2.2.9) represents the contribution of sums of wave frequency pairs to the second order response, whereas the second term gives the contribution of differences of wave frequency pairs.

Newman[20] defined the second term as slowly varying second order response.

From this result it is found that $G_2(\omega_1,-\omega_2)$ represents the property of slowly varying second order response.

2.3 Transfer Functions and Response Spectrum

2.3.1 Cross Spectrum and Auto Spectrum

Forming the cross correlation function between $x(t)$ and $\xi(t)$ from Eq. (2.1.5):

$$\begin{aligned}E\{(x(t)-\bar{x})\xi(t-\tau)\}&=\int_{\tau_1}d\tau_1 g_1(\tau_1)E\{\xi(t-\tau_1)\xi(t-\tau)\}\\&\quad+\int_{\tau_1}d\tau_1\int_{\tau_2}d\tau_2 g_2(\tau_2,\tau_2)E\{(t-\tau_1)\\&\quad\times\xi(t-\tau_2)\xi(t-\tau)\}-\bar{x}\,E\{\xi(t-\tau)\}\end{aligned} \tag{2.3.1}$$

Because the wave is defined to be zero-mean, the last two terms are zero. Thus:

$$E\{(x(t)-\bar{x})\zeta(t-\tau)\}=\int_{\tau_1} d\tau_1 g_1(\tau_1) E\{\zeta(t-\tau_1)\zeta(t-\tau)\} \tag{2.3.2}$$

This result means that the cross spectrum between response $x(t)$ and wave $\zeta(t)$ involves only the first (linear) term of the functional polynomials, and thus that the linear transfer function $G_1(\omega)$ is derivable by standard cross-spectral technique. If the cross spectrum is denoted as $S_{x\zeta}(\omega)$; then:

$$G_1(\omega)=S_{x\zeta}(\omega)/S_\zeta(\omega) \tag{2.3.3}$$

Forming the auto correlation function of $x(t)$:

$$\begin{aligned} E\{(x(t)-\bar{x})(x(t+\tau)-\bar{x})\}&=\int_{\tau_1} d\tau_1 \int_{\tau_2} d\tau_2 g_1(\tau_1) g_1(\tau_2) \\ &\times E\{\zeta(t-\tau_1)\zeta(t+\tau-\tau_2)\} \\ &+\int_{\tau_1} d\tau_1 \cdots\cdots \int_{\tau_4} d\tau_4 g_2(\tau_1, \tau_2) g_2(\tau_3, \tau_4) \\ &\times E\{\zeta(t-\tau_1)\zeta(t-\tau_2)\zeta(t+\tau-\tau_3)\zeta(t+\tau-\tau_4)\}-\bar{x}^2, \end{aligned} \tag{2.3.4}$$

and using the factorization relation for higher-order moments of Gaussian process as

$$\begin{aligned} E\{X_1X_2X_3X_4\}&=E\{X_1X_2\}\ E\{X_3X_4\}+E\{X_1X_3\}\ E\{X_2X_4\} \\ &+E\{X_1X_4\}\ E\{X_2X_3\}, \end{aligned} \tag{2.3.5}$$

we obtain

$$\begin{aligned} R_{xx}(\tau)&=\int_{\tau_1} d\tau_1 \int_{\tau_2} d\tau_2 g_1(\tau_1) g_1(\tau_2) R_\zeta(\tau+\tau_1-\tau_2)+\int_{\tau_1} d\tau_1 \cdots\cdots \int_{\tau_4} d\tau_4 \\ &\times g_2(\tau_1, \tau_2) g_2(\tau_3, \tau_4)\{R_\zeta(\tau+\tau_1-\tau_3) R_\zeta(\tau+\tau_2-\tau_4) \\ &+R_\zeta(\tau+\tau_1-\tau_4) R_\zeta(\tau+\tau_2-\tau_3)\}. \end{aligned} \tag{2.3.6}$$

The auto power spectrum of $x(t)$ is the Fourier transform of $R_{xx}(\tau)$ and is computed from Wiener-Khintchine relations as

$$\begin{aligned} S_x(\omega)&=|G_1(\omega)|^2 S_\zeta(\omega)+2\int_{-\infty}^{\infty} d\xi |G_2(\omega-\xi, \xi)|^2 \\ &\times S_\zeta(\omega-\xi) S_\zeta(\xi). \end{aligned} \tag{2.3.7}$$

2.3.2 Cross Bispectrum

Tick[13] defined the cross bispectrum as the two dimensional Fourier transform of a third moment function $R_{\zeta\zeta x}(\tau_1, \tau_2)$ which is defined as

$$R_{\zeta\zeta x}(\tau_1, \tau_2)=E\{\zeta(t+\tau_1)\zeta(t-\tau_1)(x(t-\tau_2)-\bar{x})\}. \tag{2.3.8}$$

Noting that the expected value of odd products of Gaussian variable are zero, then :

$$R_{\xi\xi x}(\tau_1, \tau_2) = 2\int_{t_1} dt_1 \int_{t_2} dt_2 g_2(t_1, t_2) R_\xi \{t_1 + (\tau_1 + \tau_2)\} R_\xi \{t_2 + (\tau_2 - \tau_1)\} \tag{2.3.9}$$

Utilizing Parseval's formula and the relation in which cross bispectrum is defined by the double Fourier transform of $R_{\xi\xi x}$, we obtain

$$C_{\xi\xi x}(\omega_1 - \omega_2, \omega_1 + \omega_2) = G_2^*(\omega_1, \omega_2) S_\xi(\omega_1) S_\xi(\omega_2), \tag{2.3.10}$$

where $C_{\xi\xi x}$ is the cross bispectrum and $*$ denotes the complex conjugate. Thus the quadratic transfer function is obtained from (2.3.10) as

$$G_2(\omega_1, \omega_2) = C^*_{\xi\xi x}(\omega_1 - \omega_2, \omega_1 + \omega_2) / S_\xi(\omega_1) S_\xi(\omega_2). \tag{2.3.11}$$

2.4 Instantaneous Probability Density Function

We shall consider the distribution of the time invariant quadratic system subject to a stationary Gaussian excitation.

If the system is represented by Eq. (2.1.5), then from Appendix A the characteristic function can be written as

$$\phi(\theta) = \prod_{j=1}^{\infty} \phi_j(\theta) = \prod_{j=1}^{\infty} (1 - 2i\lambda_j\theta)^{-1/2} \exp\{-c_j^2\theta^2/2(1 - 2i\lambda_j\theta)\}. \tag{2.4.1}$$

Since the instantaneous probability density function is defined by the Fourier transform of the characteristic function, it becomes

$$p_x(x) = 1/2\pi \int_{-\infty}^{\infty} d\theta \exp(-i\theta x) \phi(\theta), \tag{2.4.2}$$

where λ_j are real eigenvalues given by the following integral equation

$$\int_{-\infty}^{\infty} d\nu S_\xi(\omega) G_2(\omega, -\nu) \Psi_n(\nu) = \lambda_n \Psi_n(\omega), \tag{2.4.3}$$

where $\Psi_n(\omega)$ are the eigenfunctions satisfying the orthogonal relation as

$$\int_{\omega_1} d\omega_1 \int_{\omega_2} d\omega_2 \Psi_n(\omega_1) \Psi_m(\omega_2) G_2(-\omega_1, -\omega_2) = \lambda_n \delta_{mn}. \tag{2.4.4}$$

The parameter c_j representing the linear response can be obtained from

$$c_j = \int_\omega d\omega G_1(\omega) \Psi_j(\omega). \tag{2.4.5}$$

From Appendix B the statistical values up to third order can be obtained as

$$E\{x\} = \sum_{i=1}^{\infty} \lambda_i = \int_\omega d\omega G_2(\omega, -\omega) S_\xi(\omega), \tag{2.4.6}$$

$$\sigma_x^2 = \sum_{i=1}^{\infty} c_i^2 + 2\sum_{i=1}^{\infty} \lambda_i^2 = \int_\omega d\omega |G_1(\omega)|^2 S_\xi(\omega) + 2\int_\omega d\omega \int_\nu d\nu |G_2(\omega, \nu)|^2 S_\xi(\omega) S_\xi(\nu), \tag{2.4.7}$$

$$\mu\sigma_x^3 = 8\sum_{i=1}^{\infty} \lambda_i^3 + 6\sum_{i=1}^{\infty} c_i^2 \lambda_i = 8\int_{\omega_1} d\omega_1 \int_{\omega_2} d\omega_2 \int_{\omega_3} d\omega_3 G_2(\omega_1, \omega_2)$$

$$\times G_2^*(\omega_2,\omega_3)\,G_2(\omega_3,\,-\omega_1)\,S_\zeta(\omega_1)\,S_\zeta(\omega_2)\,S_\zeta(\omega_3)+6\int_{\omega_i}d\omega_1\int_{\omega_2}d\omega_2$$
$$\times G_1(-\omega_1)\,G_1(-\omega_2)\,G_2(\omega_1,\,\omega_2)\,S_\zeta(\omega_1)\,S_\zeta(\omega_2), \qquad (2.4.8)$$

where σ_x^2 and μ are the variance and the skewness of $x(t)$, respectively.

Eqs.(2.4.6), (2.4.7) and (2.4.8) show the most important relations between the transfer functions of second order response and statistical values.

2.5 Probability Density Functions of Extremal Values and Extreme value

2.5.1 Probability Density Function of Extremal Values

First we will define that the extremal values consist of the maxima and the minima of a random process while the extreme value is the largest value of the maxima or the minima that will occur in some observations.

It has been known that statistical prediction of the extremal values of a random process may be made by using the Rayleigh distribution, if the following conditions are satisfied:

1) Random process is a stationary Gaussian process with zero mean.

2) Extremal values are statistically independent.

3) Linearity must hold between input and output processes.

But since in the case of the horizontal response of a moored floating structure the linearity is not satisfied as described in the previous section, the Rayleigh distribution may no longer be applicable for predicting properties of the extremal values. Thus, the new prediction method of probability density function of extremal values is required.

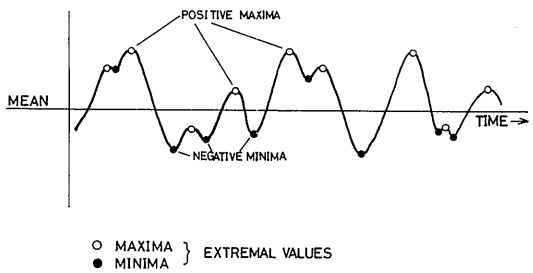

Fig. 1 Explanatory sketch of a random process $x(t)$

Fig. 1 is an explanatory sketch of a random process $x(t)$ for which the extremal values could be anywhere in the range of $(-\infty, \infty)$ and several extremal values could occur during one cycle as defined by mean crossings. Here, the extremal values called "maxima" are defined as peaks which satisfy the condition $\dot{x}(t)=0$ and $\ddot{x}(t)<0$. Whereas "minima" are defined as troughs satisfying the condition $\dot{x}(t)=0$ and $\ddot{x}(t)>0$. As shown in Fig. 1 maxima and minima can be both negative values and positive values. The magnitude of the

maxima with positive values $\{x(t)>0, \dot{x}(t)=0, \ddot{x}(t)<0\}$ or the minima with negative values $\{x(t)<0, \dot{x}(t)=0, \ddot{x}(t)>0\}$ would be critical if they exceed a certain value, and hence the statistical extreme values of these maxima and the minima provide valuable information for the engineering design purpose.

For the problem of a mooring system the positive maxima are the most important, if the direction drifted by waves is positive. Since the statistical properties of negative minima can be estimated from those of positive maxima by means of the transform of random variables, the latter are considered in the following analysis.

It can be assumed that $x(t)$ is stationary and zero mean without loss of generality. Then the expected number of maxima above a specified level $x(t)=\xi$, denoted as $E\{M(\xi)\}$, is obtained by

$$E\{M(\xi)\}=\int_{\xi}^{\infty}dx\int_{-\infty}^{0}|\ddot{x}|\,p_{x\dot{x}\ddot{x}}(x, 0, \ddot{x})\,d\ddot{x}. \tag{2.5.1}$$

The expected number of maxima with positive values, denoted as $E\{M(0)\}$, then becomes

$$E\{M(0)\}=\int_{0}^{\infty}dx\int_{-\infty}^{0}|\ddot{x}|\,p_{x\dot{x}\ddot{x}}(x, 0, \ddot{x})\,d\ddot{x}, \tag{2.5.2}$$

where $p_{x\dot{x}\ddot{x}}$ is the joint probability density function of x, $\dot{x}$ and $\ddot{x}$.

Huston and Skopinski[15] has assumed that the ratio of their two expected number is approximately equivalent to the probability in which the maximum values exceed a level ξ.

Under this assumption the probability in which the maximum positive values exceed a level ξ becomes

$$P_p(\xi)=1-E\{M(\xi)/M(0)\}\sim 1-E\{M(\xi)\}/E\{M(0)\}. \tag{2.5.3}$$

Then the probability density function of the maxima is given by

$$p_p(\xi)=-\frac{1}{E\{M(0)\}}\int_{-\infty}^{0}d\ddot{x}\;\ddot{x}p_{x\dot{x}\ddot{x}}(\xi, 0, \ddot{x}). \tag{2.5.4}$$

In the case that $x(t)$ is the Gaussian process p_p already has been obtained by Cartwright and Longuet Higgins[16]. But in the case of nonlinear response p_p has not been found out yet.

When $x(t)$ is narrow banded, Powell[17] has proposed the following assumptions:

1) The response is narrow banded. That is, the negative maxima and the positive minima are negligible.
2) The response is stationary.
3) The random number crossing a specified level at positive gradient is equal to one of maxima above it.

Here, the random number crossing a specified level ξ at positive gradient is

defined as

$$N^+(\xi)=\dot{x}\delta(x-\xi). \tag{2.5.5}$$

From these assumptions

$$M(\xi)\simeq N^+(\xi). \tag{2.5.6}$$

Thus, Eq. (2.5.4) becomes

$$p_p(\xi)\simeq\frac{-1}{E\{M(0)\}}\cdot\frac{d}{d\xi}\int_0^\infty d\dot{x}p_{x\dot{x}}(\xi,\dot{x})\dot{x}, \tag{2.5.7}$$

where $p_{x\dot{x}}$ is the joint probability density function of x and $\dot{x}$.

Powell also indicated these assumptions can even be applied to the case in which the response is wide banded. Because the positive minima and the negative maxima are negligible since these values do not exist at which the threshold level is sufficiently large.

In general, since $E\{M(0)\}\geqq E\{N^+(0)\}$, the probability of maxima is overestimated in Powell's assumptions.

2.5.2 Extreme Value

In this section, the extreme value will be derived by applying the order statistics. The extreme value defined here is the largest value of the maxima that will occur in N observations.

Let $(y_1, y_2, \cdots\cdots, y_N)$ be an ordered sample of size N, where y_i is the observed maxima of a random process $x(t)$, then all y_i have the same probability density function given in (2.5.7). Let $(\eta_1, \eta_2, \cdots\cdots, \eta_N)$ be an ordered sample of y_i with $\eta_1\leqq\eta_2\leqq\cdots\cdots\leqq\eta_N$, then each η_i can be regarded as the output of a independent random variable z_i. Thus the random variable z_N, which is the largest η_N in the ordered sample, has the following probability density function:

$$g(\eta_N)=Nf(\eta_N)\ \{F(\eta_N)\}^{N-1}, \tag{2.5.8}$$

where

$g(\eta_N)$: Probability density function of the largest value in N observations,

$f(\eta_N)$: Probability density function given by replacing ξ with η_N in Eq. (2.5.7),

$F(\eta_N)$: Cumulative distribution function given by integrating Eq. (2.5.7) with respect to ξ and replacing ξ with η_N,

N: The number of observations.

Thus the extreme value estimate is obtained by

$$E\{z_m\}=\int_0^\infty d\eta_N\eta_N g(\eta_N). \tag{2.5.9}$$

3. APPROXIMATE THEORY

3.1 Approximation to the Quadratic Transfer Function

If the horizontal response of a moored floating structure is expressed by (2.1.5) the second term in Eq. (2.1.5) represents the response which is in proportion to the squared wave height, that is, instantaneous wave energy. The authors[18] have introduced the linear response function g between the horizontal response and the instantaneous wave energy, and have shown that g is approximately equivalent to the quadratic transfer function. Here, we shall quote their results.

The cross correlation function $R_{x\zeta^2}$ between the instantaneous wave energy $\zeta^2(t)$ and the second order nonlinear response $x(t)$ is defined by

$$R_{x\zeta^2}(\tau)=E\ \{(x(t)-\bar{x})(\zeta^2(t+\tau)-\bar{\zeta}^2)\}. \tag{3.1.1}$$

Applying Parseval's formula, the cross spectrum $S_{x\zeta^2}$ is given by

$$S_{x\zeta^2}(\omega)=2\int_\nu d\nu S_\zeta(\omega-\nu)S_\zeta(\nu)G_2^*(\omega-\nu,\ \nu), \tag{3.1.2}$$

and the auto power spectrum of instantaneous wave energy is obtained from

$$S_E(\omega)=2\int_\nu d\nu S_\zeta(\omega-\nu)S_\zeta(\nu). \tag{3.1.3}$$

Thus, g representing the response property between the instantaneous wave energy and $x(t)$ is given as follows:

$$g=\int_\nu d\nu S_\zeta(\omega-\nu)S_\zeta(\nu)G_2^*(\omega-\nu,\ \nu)\Big/\int_\nu d\nu S_\zeta(\omega-\nu)S_\zeta(\nu) \tag{3.1.4}$$

From Eq. (3.1.4) it is found that g indicates the average of G_2 with respect to the instantaneous wave energy spectrum and depends on the wave spectral density. If the following identity

$$\int_{\omega_i} d\omega_1\int_{\omega_2} d\omega_2\, g(\omega_1)S_\zeta(\omega_1-\omega_2)S_\zeta(\omega_2) = \int_{\omega_i} d\omega_1\int_{\omega_2} d\omega_2 S_\zeta(\omega_1-\omega_2)S_\zeta(\omega_2)G_2^*(\omega_1-\omega_2,\ \omega_2) \tag{3.1.5}$$

is satisfied, we obtain

$$g^*(\omega_1+\omega_2)\simeq G_2(\omega_1,\ \omega_2). \tag{3.1.6}$$

This means that g is approximately equal to the quadratic transfer function under a fixed wave spectrum.

If this approximation is applicable, we have

$$x(t)=\int_\tau d\tau g_1(\tau)\zeta(t-\tau)+1/\pi\int_\tau d\tau f_{\zeta^2}(\tau)\zeta^2(t-\tau), \tag{3.1.7}$$

where

$$f_{\zeta^2}(\tau)=1/2\pi\int_{\omega}d\omega\ g(\omega)\exp(i\omega\tau). \tag{3.1.8}$$

Thus the second term in (3.1.7) can be regarded as the output through a filtered square law detector and $f_{\zeta^2}(\tau)$ is interpreted as the filter impulse response.

3.2 Approximation to the Instantaneous Probability Density Function

From Appedix B the horizontal response of a moored floating structure in irregular waves is alternatively represented in the following form :

$$x=\sum_{i=1}^{\infty}(c_iX_i+\lambda_iX_i^2), \tag{3.2.1}$$

where X_i are standard Gaussian random variables with zero mean and their variances are equal to unity.

Here, we shall assume that the number of eigenvalues λ_j is finite and sufficiently large.

If we introduce the new random variables Z_i as

$$Z_i=c_iX_i+\lambda_iX_i^2, \tag{3.2.2}$$

then it is shown that Z_i and $Z_j(i\neq j)$ are mutually independent and each Z_i has the same probability density function. Thus, if the higher moments of Z_i are finite, $x(t)$ is subject to the local limit theorem[19], that is, $x(t)$ will asymptotically become Gaussian.

Now, we replace $x-\bar{x}$ by y and introduce the error function $\varepsilon(y)$ defined by

$$\varepsilon(y)=p_x(y)-1/\sqrt{2\pi\sigma_x^2}\,exp(-y^2/2\sigma_x^2). \tag{3.2.3}$$

If ε can be represented by the family of orthogonal functions with weighting function, $\{w(y)h_n(y)\}$, it can be expanded in the following form :

$$\varepsilon(y)=\sum_{n=1}^{\infty}\alpha_nh_n(y)w(y), \tag{3.2.4}$$

where h_n are the orthogonal functions and $w(y)$ is the weighting function, and where α_n are the coefficients given by

$$\alpha_n=\int_{-\infty}^{\infty}dyh_n(y)\varepsilon(y). \tag{3.2.5}$$

If $w(y)$ is the Gaussian density function it is well known that $h_n(y)$ are given by the Hermite polynomials[19].

From the properties of the Hermite polynomials the instantaneous probability density function can be approximated by the Gram-Charlier expansion[9] :

$$p_x(x)\simeq 1/\sqrt{2\pi}\sigma_x\ \{1+\sum_{n=3}^{\infty}b_n/(n!\,\sigma_x^n)H_n((x-\bar{x})/\sigma_x)\}$$
$$\times\exp\{-(x-\bar{x})^2/2\sigma_x^2\}, \tag{3.2.6}$$

where H_n are the Hermite polynomials and b_n represent the higher moments defined by

$$b_n = E\{(x-\bar{x})^n\} \qquad for\ n \geqq 3. \tag{3.2.7}$$

From Eqs.(3.2.7) and (2.4.8) the following relation is satisfied:

$$b_3 = \sigma_x^3 \mu. \tag{3.2.8}$$

If Eq. (3.2.6) is truncated at finite order, the finite Gram-Charlier expansion can not represent the asymptotic behaviour of the probability density as $|x| \to \infty$. Thus it is necessary to investigate it from the exact solution.

We assume that λ_j can be ordered and λ_1 (max λ_j) is positive and λ_2 (min λ_j) is negative. For $x \to \infty$ the integration path of Eq. (2.4.2) can be deformed such that it goes along the branch-cuts in the left half plane and the main contribution to this integral will be that from the neighbourhood of the branch-point closest to the imaginary axis (see Appendix C).

We introduce the following function[5]:

$$\tilde{\phi}(\theta) = (1-2i\lambda_1\theta)^{-1/2} \exp\{-c_1^2\theta^2/2(1-2i\lambda_1\theta)\} \prod_{j=2}^{\infty} \phi_j(-i/2\lambda_1) \tag{3.2.9}$$

Since $\phi/\tilde{\phi}$ is analytical in the vicinity of the branch point closest to the imaginary axis, the first approximation to $p_x(x)$ can be found as

$$p_x(x) \simeq 1/2\pi \int_{-\infty}^{\infty} d\theta \tilde{\phi}(\theta) \exp(-i\theta x) \prod_{j=2}^{\infty} \phi_j(-i/2\lambda_1). \tag{3.2.10}$$

Since $(Z_1/\lambda_1 + c_1^2/4\lambda_1^2)$ is of non-central χ^2 distribution with one degree of freedom, the following form[5] is found out by means of the asymptotic expansion of the non-central χ^2 distribution as $x \to \infty$:

$$p_x(x) \simeq 1/\sqrt{2\pi\lambda_1 x} \exp\{-(x+c_1^2/2\lambda_1)/2\lambda_1\} \cosh(\sqrt{x/\lambda_1} c_1/2\lambda_1) \tag{3.2.11}$$

The same expression can easily be derived for $x \to -\infty$.

These results show that x/λ_1 is asymptotically of χ^2 distribution with one degree of freedom and with a slight modification caused by the linear term.

If the second term in (2.1.5) is dominant, from Appendix C we get:

$$p_x(x) \simeq 1/2\pi \sqrt{\lambda_1|\lambda_2|} \exp\{(\lambda_1 - |\lambda_2|)x/4\lambda_1|\lambda_2|\} \times K_0\{|x|(\lambda_1+|\lambda_2|)/4\lambda_1|\lambda_2|\} \qquad as\ |x| \to \infty \tag{3.2.12}$$

where K_0 is the modified Bessel function of the second kind.

Thus, the approximate solution for the instantaneous probability density function will be obtained by matching between the finite Gram-Charlier expansion and the asymptotic form derived from the exact solution.

3.3 Approximation to the Probability Density Function of Extremal Values

By expanding the one dimensional Gram-Charlier expansion to the two dimensional form joint probability density funcion of x and $\dot{x}$ can be approximately represented in the following form:

$$p_{x\dot{x}}(x,\dot{x}) = 1/2\pi\sigma_x\sigma_{\dot{x}} \exp\{-(x-\bar{x})^2/2\sigma_x^2 - \dot{x}^2/2\sigma_{\dot{x}}^2\} \sum_{m,n} b_{mn} \times H_m\{(x-\bar{x})/\sigma_x\} H_n(\dot{x}/\sigma_{\dot{x}}), \tag{3.3.1}$$

where b_{mn} is a function of the higher moments of x and $\dot{x}$.

The above equation is called "two dimensional Gram-Charlier expansion" and is equivalent to the results given from the series expansion of cumulants by Vinje[4].

In the case of the nonlinear response, x and $\dot{x}$ are not mutually independent even though x is stationary. But since the low frequency response of a moored floating structure is limited in the low frequency regions, it will be expected that the contribution of the low frequency response to the motion velocity is very small. Thus $\dot{x}$ may be expressed as

$$\dot{x} \simeq \int_\tau d\tau g_1(\tau)\dot{\xi}(t-\tau), \tag{3.3.2}$$

where dots denote time derivatives.

Since the surface elevation $\zeta(t)$ is assumed to be the stationary Gaussian process with zero mean, $\zeta(t)$ and $\dot{\zeta}(t)$ are mutually independent.

Since it will be proper to assume that $\dot{x}$ is Gaussian distributed and x and $\dot{x}$ are mutually independent,

we obtain the following form:

$$p_{x\dot{x}}(x,\dot{x}) \simeq 1/2\pi\sigma_x\sigma_{\dot{x}}\{1+\sum_n b_n/(n!\,\sigma_x^n) H_n\{(x-\bar{x})/\sigma_x\} \times \exp\{-(x-\bar{x})^2/2\sigma_x^2 - \dot{x}^2/2\sigma_{\dot{x}}^2\}, \tag{3.3.3}$$

where $\bar{x}$ and σ_x^2 are the mean and the variance of $x(t)$ respectively and $\sigma_{\dot{x}}^2$ is the variance of $\dot{x}$.

Then replacing ξ by $\eta+\bar{x}$ in Eq. (2.5.7), the probability density function of maxima can be represented as:

$$p_p(\eta) = -\{-\eta/\sigma_x^2 \exp(-\eta^2/2\sigma_x^2)\{1+\sum_n b_n/(n\,!\,\sigma_x^n) H_n(\eta/\sigma_x)\} + \exp(-\eta^2/2\sigma_x^2)\sum_n b_n/(n!\sigma_x^{n+1}) H_n'(\eta/\sigma_x)\} \times\{1+\sum_n b_n/(n!\sigma_x^n) H_n(0)\}^{-1} \tag{3.3.4}$$

This means that p_p is equivalent to the derivative form of Eq. (3.2.6). Thus p_p for some sufficient large η will asymptotically approach to the following form:

$$p_p \sim -d/d\eta \{\sqrt{\bar{x}/(\bar{x}+\eta)}\exp(-\eta/2\lambda_1)\cosh\{\sqrt{(\eta+\bar{x})/\lambda_1}(c_1/2\lambda_1)\} /\cosh\{\sqrt{\bar{x}/\lambda_1}(c_1/2\lambda_1)\}\} \tag{3.3.5}$$

If the low frequency motion is dominant, the asymptotic form for $\eta \to \infty$

is given as follows :

$$p_p \sim -d/d\eta \left[\exp\{(\lambda_1-|\lambda_2|)/4\lambda_1|\lambda_2|\}\right.$$
$$\times K_o\{(\eta+\bar{x})(\lambda_1+|\lambda_2|)/4\lambda_1|\lambda_2|\}$$
$$\left./K_o\{\bar{x}(\lambda_1+|\lambda_2|)/4\lambda_1|\lambda_2|\}\right] \qquad (3.3.6)$$

Using Eqs. (3.3.5) of (3.3.6) the extreme responses can be obtained from Eq. (2.5.9).

4. COMPARISONS BETWEEN STATISTICAL ESTIMATIONS AND EXPERIMENTAL RESULTS

4.1 Model Test

4.1.1 Configuration of Model

The model used in the test and the co-ordinate system are shown in Fig.2 and the principal dimensions of the model are given in Table 1.

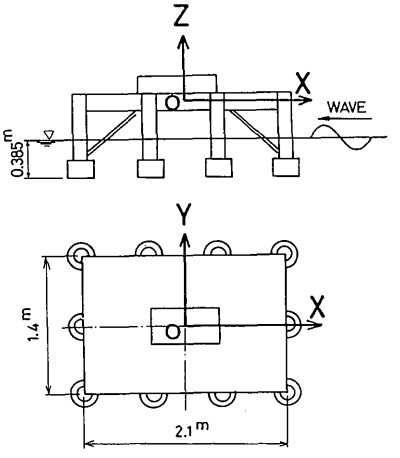

Fig. 2 Configuration of offshore structure and system of coordinate

Table. 1 Principal dimensions

ITEMS	ACTUAL	MODEL
LENGTH (m)	30.0	2.1
BREADTH (m)	20.0	1.40
DISPLACEMENT (t)	490.0	0.168
DRAFT (m)	5.5	0.385
KG (m)	4.758	0.330
Kyy	42.6%L	44%L
GM_L (m)	3.845	0.269
SCALE RATIO	1.0	1/14.3
MOORING	CATENARY	LINEAR SPRING

4.1.2 Model Test and Measurement Items

The long duration measurements in irregular waves are required for the low frequency surge motions to get the reliable data in statistics.

Furthermore, the data obtained must contain a number of oscillations with randomness at the frequencies of interest. Therefore, in order to generate the irregular waves over long duration the filtered signals were used, which were obtained by passing the white noize signals generated from a noize generator into the bandpass filter. The rolloff (the cutoff characteristics) of the bandpass filter was 24db/oct.. Besides, regular waves and amplitude modulation waves

were also used to investigate the steady drift displacement and the quadratic transfer function of surge motions.

Four kinds of irregular waves were generated. The central frequencies f_0 of the bandpass filter used for the generation of each waves were 0.4, 0.5, 0.6, and 0.7Hz. These frequencies correspond to 9.45, 7.56, 6.30, and 5.40 sec. respectively in the scale of real structures.

In the case of $f_0=0.7$Hz the duration time was about 5.7hr in real scale, and for the other cases it was about 2.8hr. The model tests were carried out at the Mitaka No. 2 Ship Experimental Tank (400m in length, 18m in breadth, 8m in depth) in Ship Research Institute. The test set-up is shown in Fig. 3.

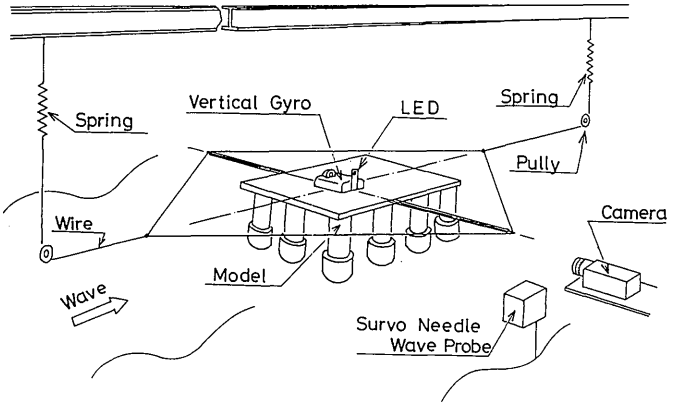

Fig. 3 Set-up of model test

As shown in Fig. 3, the model was restrained by two soft springs through the device which restricted the yaw motion. Their spring coefficients were 1.683 kg/m. The encounter angle to waves was zero degree.

The measured items are as follows:

-Surge and heave motion measured by the optical motion measuring system using L. E. D.;

-Pitch motion measured by the vertical gyroscope;

-Surface elevation measured by the servo needle wave probe fixed at a position, the x coordinate of which is equal to that of the centre of gravity of the model in still water.

4.2 The Investigation to Irregular Waves

The spectra of irregular waves generated are shown in Fig. 4, where f_0 denotes the centre frequency of bandpass filter used for generating the irregular waves and $\tilde{\sigma}_w^2$ are the estimated variances obtained by integrating the wave spectra with respect to the wave frequency.

The Blackman-Tukey method was used in the spectral analysis, in which the

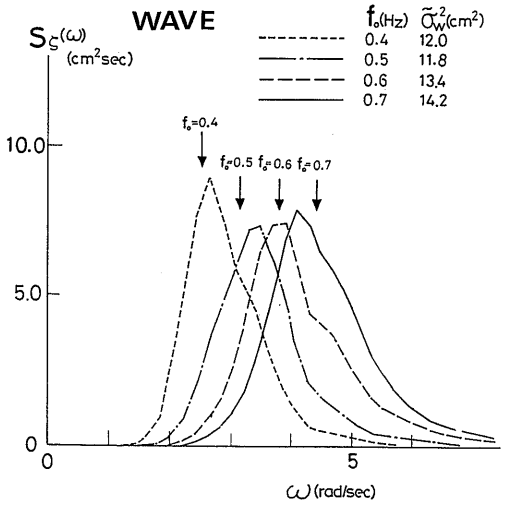

Fig. 4 Wave spectra

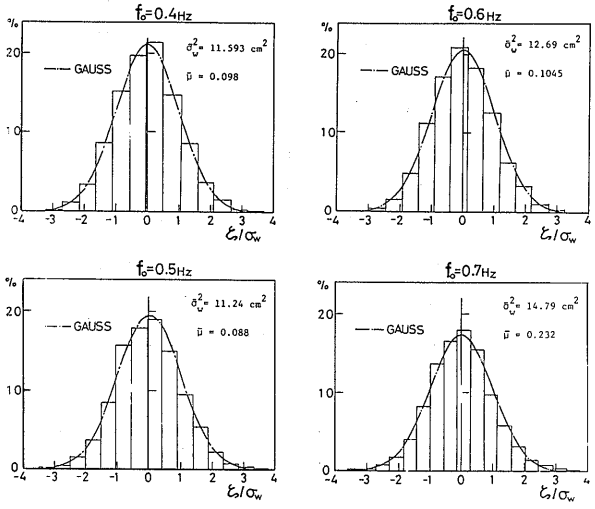

Fig. 5 Comparisons between observed histograms and Gaussian probability distributions

number of lags was 256 and the window used was the Hamming type. The number of data used for the analysis was about 45000 in the case of $f_0=0.7$Hz, and it was about 23000 in the other cases. The sampling interval was 60 msec. in all cases. Fig. 5 shows the instantaneous probability distributions of waves. In Fig. 5 $\bar{\sigma}_w^2$ and $\bar{\mu}$ is the sample variance and the sample skewness given from the time average respectively.

From Figs. 4 and 5 it is found that the spectrum shapes are different from the standard wave spectra as the I. S. S. C type or the JONSWAP type, which have the narrow band spectra.

χ^2 tests were carried out to test the hypothesis that the wave is of Gaussian process. From these results it has been found that this hypothesis is acceptable at significant level of 0.05.

Next, we shall investigate whether the random phases of waves are strongly homogeneous and uniformly distributed.

In general, even though the wave $\zeta(t)$ satisfies the Ergodicity, ζ^2 corresponding to the instantaneous wave energy does not always satisfy it.

This means that the correlation function of $\zeta^2(t)$ can not be obtained from the time average, that is, the correlation function of ζ^2 obtained from the time average is the sample function because it depends on the random phases of waves, and also the spectrum is the sample. But if the random phases of waves are homogeneous, it may be considered that the time average correlation function represents the average value in the sample functions, or the closest value to the ensemble average.

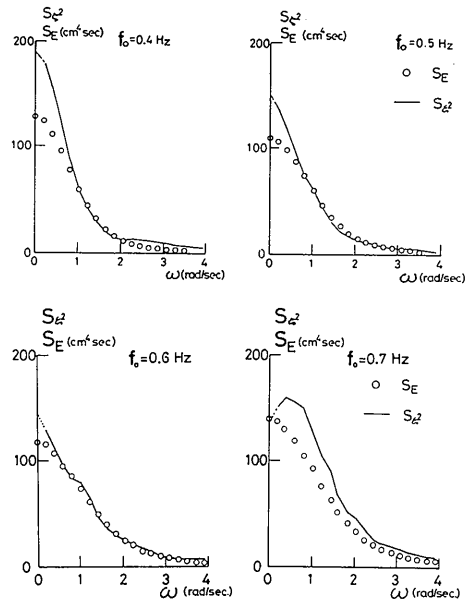

Fig. 6 Comparisons between slowly instantaneous wave energy spectra obtained from time average and their true spectra

Thus we compare the spectrum S_{ζ^2} which is given from the time average correlation function of ζ^2 with the true spectrum S_E defined in Eq. (3.1.3). These results are shown in Fig. 6. From Fig. 6 it is found that both spectra are in good agreement except for the vicinity of $\omega=0$. Accordingly it may be assumed that the random phases of waves are nearly homogeneous.

4.3 Investigation to Transfer Functions

The surge spectra given in the same manner as the wave spectra are shown in Fig. 7. From this figure it is found that the surge response in the case of $f_0=$ 0.7Hz is the largest and responses are dominated by the low frequency motion. Fig. 8 shows the linear transfer function G_1 obtained from the standard cross spectral analysis between the surge motions and the waves. In this figure the solid line represents the theoretical value due to the usual linear motion prediction method which takes into account of the viscous damping[21]. From this figure it is found that the theoretical value is in good agreement with the experimental results.

Thus it is considered that only the linear response can be separated from the surge response including the low frequency motion in the frequency domain.

In order to get the quadratic transfer function of the response the cross

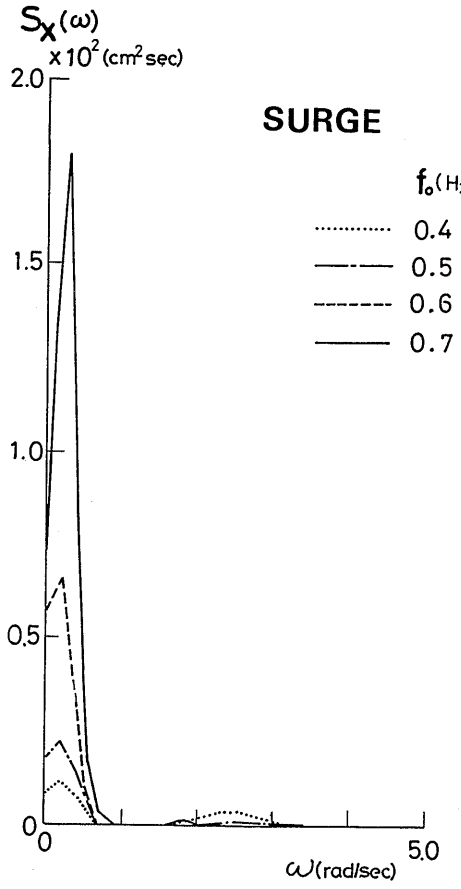

Fig. 7 Surge spectra

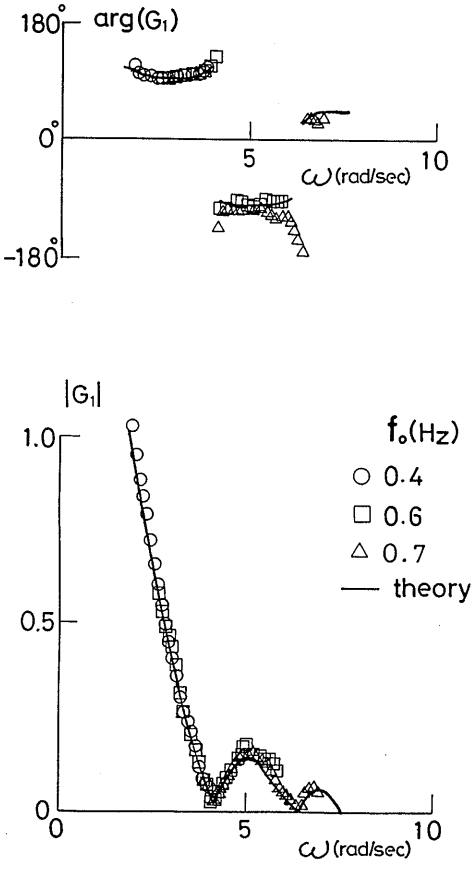

Fig. 8 Linear transfer function (G_1 (ω)) of surge motion

bispectrum between the waves and the surge motions is required. The utilization of the Fast Fourier Transform (F. F. T) has significant advantage in the computation of the full cross bispectrum. For the present purpose, however, the full computation is not required, because we need only the results on or near $\omega_1 = \omega_2$.

Accordingly we used the method developed by Dalzel[2]. The window function used in the computation of the cross bispectrum was the Hamming type extended to two dimensions. Fig. 9 shows a part of the results of the cross bispectrum.

The quadratic transfer function obtained from the experiments in amplitude modulation waves (A. M. waves) and irregular waves is shown in Fig. 10. This function in irregular waves was estimated from the cross bispectral analysis within the frequency range corresponding to the 25% power bandwidth of the wave spectrum and that in A. M. waves, which was indicated by the black

circles in the figure, was obtained from the envelope analysis[2]. For each value of the difference frequencies the amplitude parts and the phase parts of the quadratic transfer function are indicated in this figure and the abscisa is based on the mean frequency of the two wave components.

The comparisons between $G_2\ (\omega,\ -\omega)$ obtained from the experiments in irregular waves and the steady drift displacement obtained in regular waves are shown in Fig. 11. In this figure the difference between white circles and black circles indicates the effect of wave heights, and the solid line is the value obtained from the theoretical computation taking into account of the hydrodynamic interactions among floating elements under the fixed condition[22]. From Fig. 10 it is found that the result from the tests in amplitude modulation waves are in good agreement with that in irregular waves and the amplitudes of quadratic transfer function decrease with the increase of the difference frequency and the phases do not depend on the mean frequency of the two wave components. From Fig. 11 it is seen that the steady component of quadratic transfer function, $G_2\ (\omega,-\omega)$, represents the effect of wave height

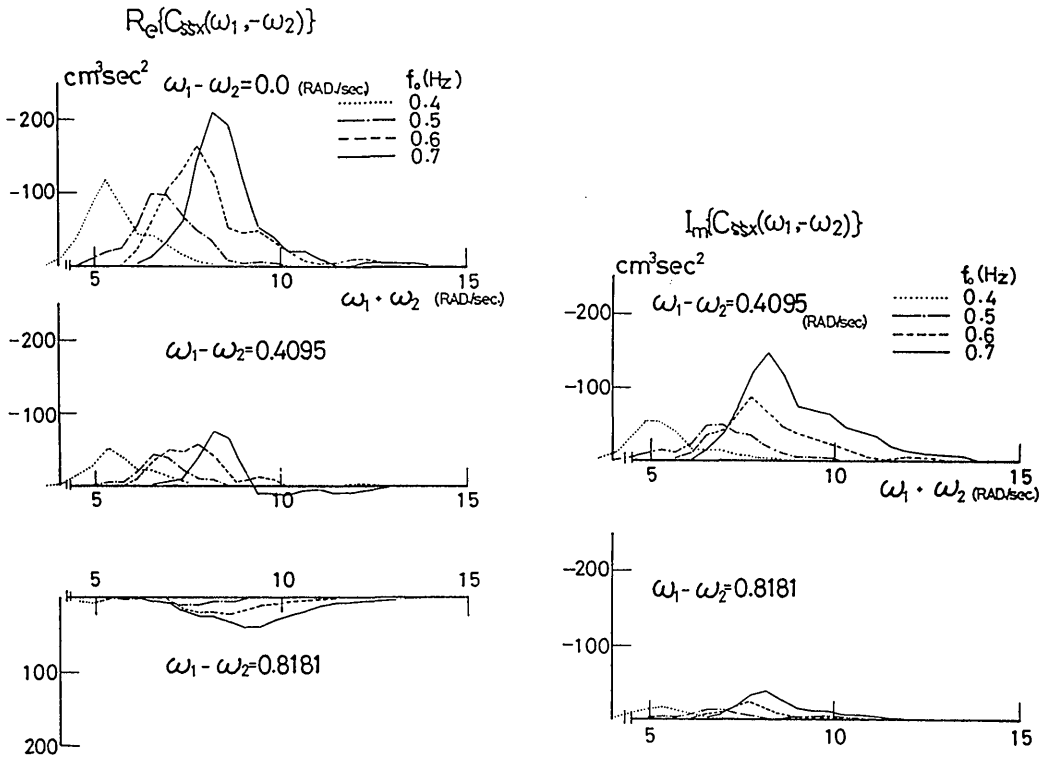

Fig. 9 Cross bispectra (wave-wave-surge)

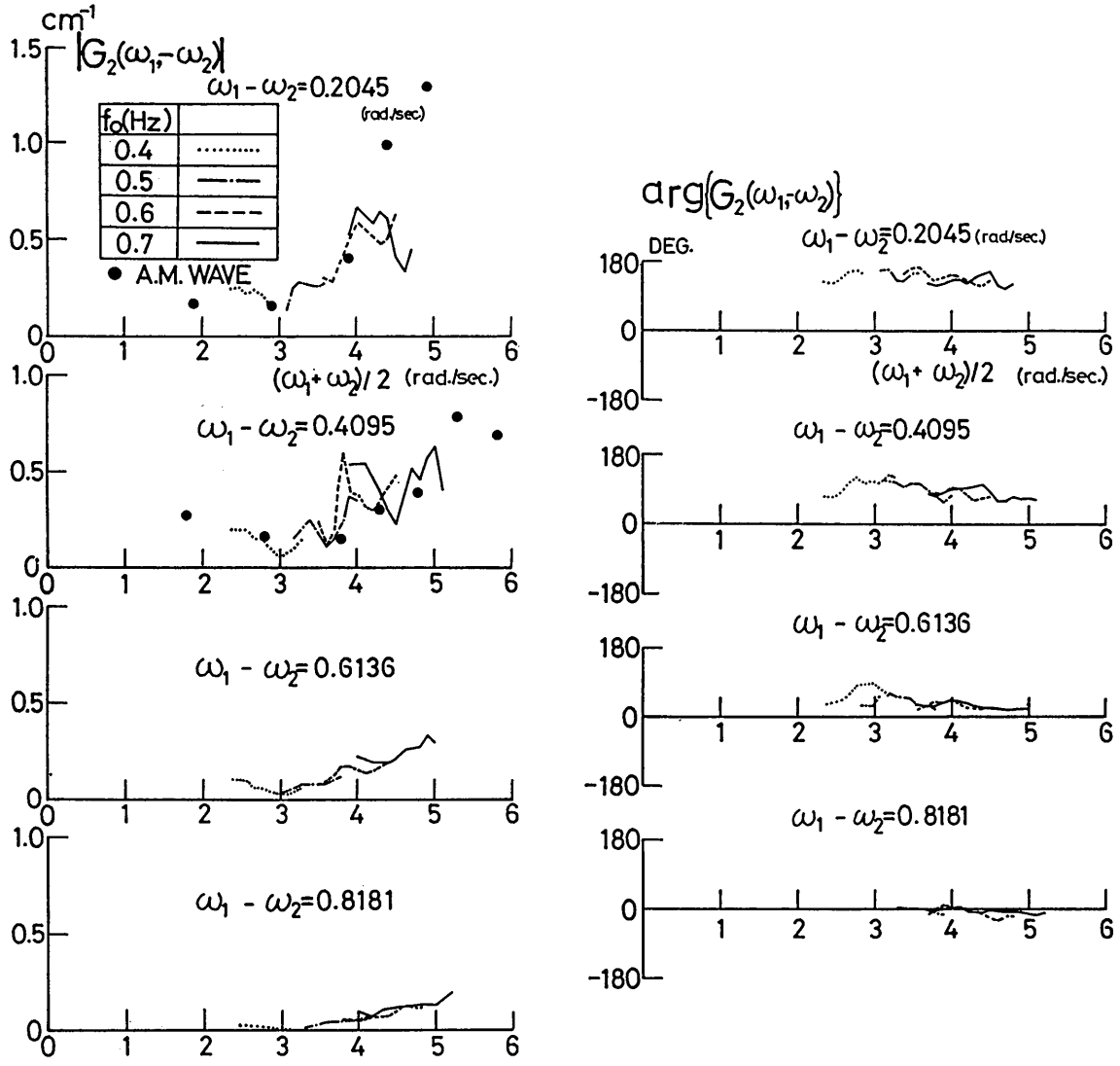

Fig. 10 Quadratic transfer function $G_2(\omega_1, -\omega_2)$ of surge motion

of the steady drift displacement in regular waves and it is not proportional to the square of wave heights.

Let $G_2^f(\omega_1, -\omega_2)$ be the quadratic transfer function of the low frequency second order force in head waves and $H_L(\omega)$ be the response function of surge motions to external forces at the low frequency motion.

Then $G_2(\omega_1, -\omega_2)$ can be represented as

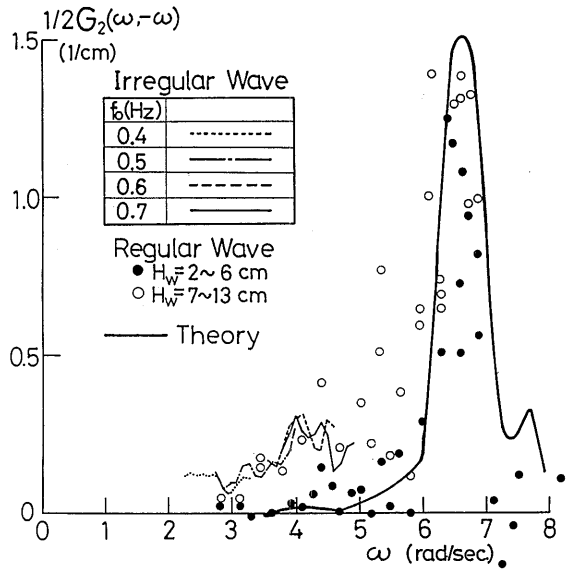

Fig. 11 Comparisons between $G_2(\omega, -\omega)$ and the steady drift excursions derived from experimental results in regular waves

$$G_2(\omega_1,-\omega_2)=G_2^f(\omega_1,-\omega_2)H_L(\omega_1-\omega_2).$$

For $G_2^f(\omega_1,-\omega_2)$ Newman[20] has suggested the following approximation:

$$G_2^f(\omega_1,-\omega_2)\simeq G_2^f(\omega_1,-\omega_1) \tag{4.3.2}$$

This means that $G_2^f(\omega_1,-\omega_2)$ can be replaced by the diagonal components of a matrix of quadratic transfer function of low frequency second order force.

Since H_L consists of the mass coefficient, the damping coefficient and the restoring force coefficient at low frequency motion, the additional components of hydrodynamic forces caused by encounter waves may be contained in H_L.

If the relation (3.1.6) is satisfied, H_L can be represented in the following form:

$$\bar{H}_L(\omega)=g^*(\omega)/g(0)=H_LK, \tag{4.3.3}$$

where K is the linear restoring force coefficient and g is the response function obtained from standard cross spectral analysis between surge motions and squared surface elevations. $\bar{H}_L$ is the non-dimensional form of H_L.

The properties of g obtained from exprimental data in irregular waves are shown in Fig. 12. In this figure the marks indicate the results obtained from G_2 by use of (3.1.6). From Fig. 12 it is found that both results agree well except for

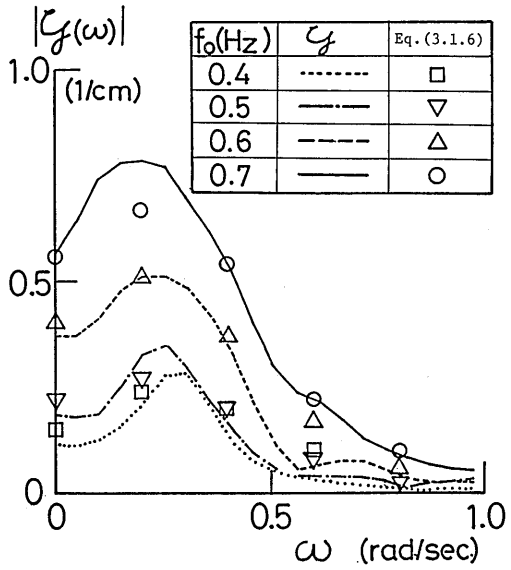

Fig. 12 Transfer function of surge motion to slowly instantaneous wave energy

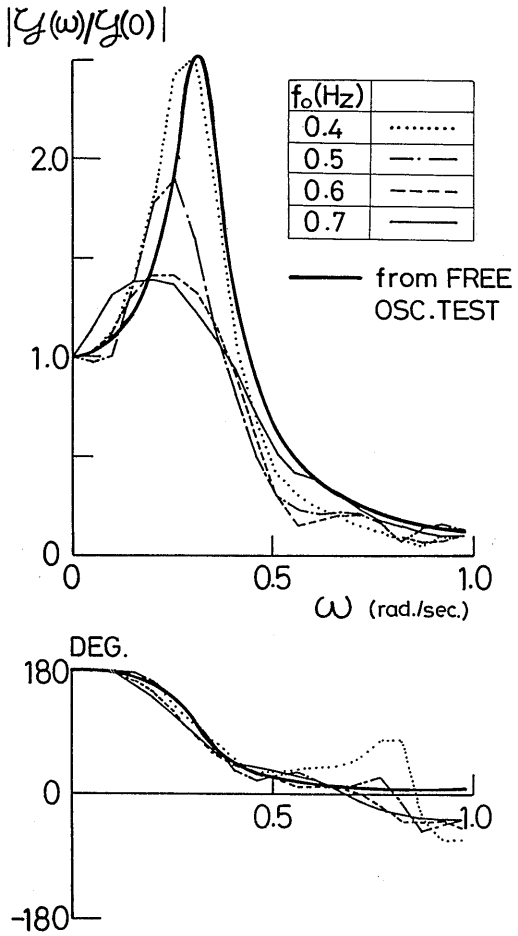

Fig. 13 Linear transfer function H_L of surge motion to external force at low frequency motion

the vicinity of peaks. Thus it is considered that the relation (3.1.6) is approximately satisfied in this case. $\bar{H}_L$ estimated from under Newman's approximation and $\tilde{H}_L$ obtained from a free oscillation test in still water are compared in Fig. 13. From this figure it is found that both results have a same tendency in terms of the characteristics of frequency, but that the natural frequency of $\bar{H}_L$ is shifted towards low frequency side in comparison with that of $\tilde{H}_L$ and the damping coefficient of $\bar{H}_L$ is larger than that of $\tilde{H}_L$, and that in particular these phenomena are remarkable when the peak frequency of wave spectrun becomes high. However since $\tilde{H}_L$ overestimates $\bar{H}_L$, it is concluded that the quadratic transfer function of surge motions, G_2, can be predicted from g by taking into account of the effect of wave heights for the steady drift displacement and by using the frequency response function of surge motions obtained from a free

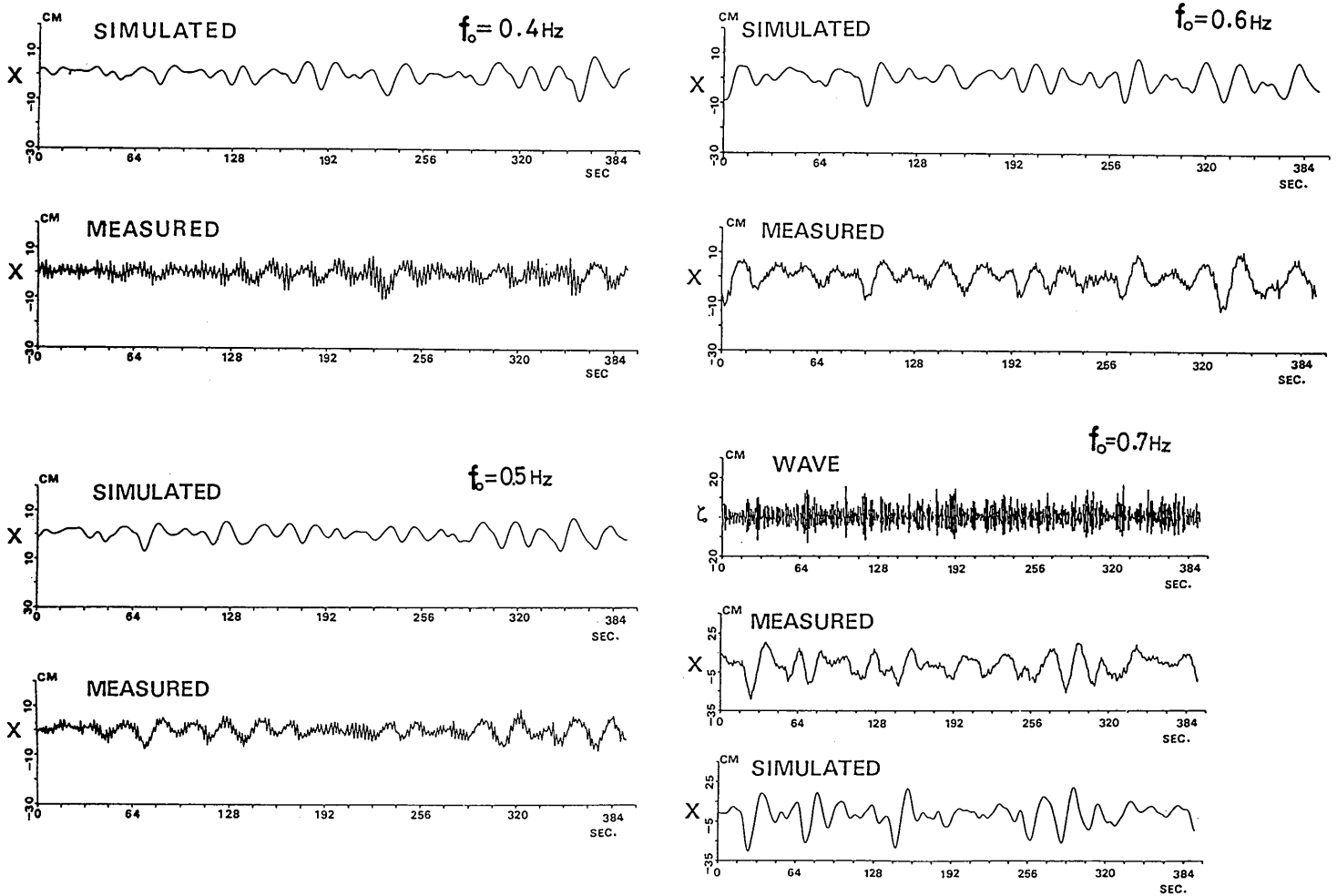

Fig. 14 Comparisons in time domain between simulated low frequency motions and measured results of surge motion

oscillation test in still water.

We shall check this fact in time domain. The result simulated by using the above results and the measured result are compared in Fig. 14. From this figure it is confirmed that the above approximation is applicable in this case.

Finally, the following results are derived within the range of this experiment:

1) The low frequency motion is dominant in the total surge motion;
2) $G_2(\omega, -\omega)$ which represents the steady drift displacement is not proportional to the square of wave heights;
3) The response function g of surge motions to the instantaneous wave energy, which is introduced newly, is approximately equal to the quadratic transfer function of surge motions;
4) The frequency response function of surge motions to external forces, H_L, is approximated by the response function obtained from a free oscillation test in still water;
5) The linear transfer function of surge motions, G_1, can be estimated from the usual linear motion prediction method and does not depend on the low frequency motion.

Thus the following relations can be obtained by applying these results to Eqs. (2.4.7) and (2.4.8).

$$\tilde{\sigma}_x^2 \fallingdotseq 2(\lambda_1^2+\lambda_2^2)=\int_0^\infty\int_0^\infty G_2^f(\omega,-\omega)^2 U_\zeta(\omega)\,|\,H_L(\omega-\nu)\,|^2 U_\zeta(\nu)\,d\nu d\omega \tag{4.3.4}$$

$$\begin{aligned}\tilde{\mu}\tilde{\sigma}_x^3 \fallingdotseq 8(\lambda_1^3-\lambda_2^3)=&3\int_0^\infty\int_0^\infty\{G_1^*(\omega)G_1(\nu)G_2^f(\omega,-\omega)H_L(\omega-\nu)\\&+G_1(\omega)G_1^*(\nu)G_2^f(\omega,-\omega)H_L^*(\omega-\nu)\}\,U_\zeta(\omega)U_\zeta(\nu)\,d\omega d\nu\\&+\int_0^\infty\int_0^\infty\int_0^\infty U_\zeta(\omega_1)U_\zeta(\omega_2)U_\zeta(\omega_3)G_2^f(\omega_1,-\omega_1)G_2^f(\omega_2,-\omega_2)\\&\times G_2^f(\omega_3,-\omega_3)\,\{H_L(\omega_1-\omega_2)H_L^*(\omega_2-\omega_3)H_L(\omega_3-\omega_1)\\&+C.C.\}\,d\omega_1 d\omega_2 d\omega_3\end{aligned} \tag{4.3.5}$$

Where C. C. denotes the complex conjugate of the previous term.

4.4 Investigation to the Instantaneous Probability Density Function of Response

Comparisons between the sample statistical values obtained from time average over total duration time and the estimated ones from Eqs. (4. 3. 4) and (4. 3. 5) are shown in Table2. Fig. 15 shows sample statistical values as a time function. From Table2 and Fig. 15 it is found that sample variances do not depend on the duration time and show constant values, while the sample skewnesses are distributed around the estimated values and depend on the duration one. But the longer the duration time, the smaller the variation of the

sample skewness around the estimated value. Thus it may be considered that the statistical values of surge motions including the low frequency motion can be predicted up to third order by using the present approximate theory.

The instantaneous probability distributions of surge motions are indicated in Fig. 16. In this figure the broken line is the estimated curve from the three term Gram-Charlier expansion and the solid line is that from the asymptotic solution of exact probability density function. From Fig. 16 it is found that the probability distribution is asymmetry with respect to $x=\bar{x}$ and has the tendency broadening towards the direction drifted by waves. Further it is seen that the degree of the breadth depends on the skewness of the distribution considerably. The results of the three term Gram-Chalier expansion are found to better fit the experimental results, while the results of the asymptotic solution do not well approximate the probability distribution. However, the latter results represent the behaviour of the probability distribution well at which x is significantly large. Thus it may be considered that the probability density function of surge

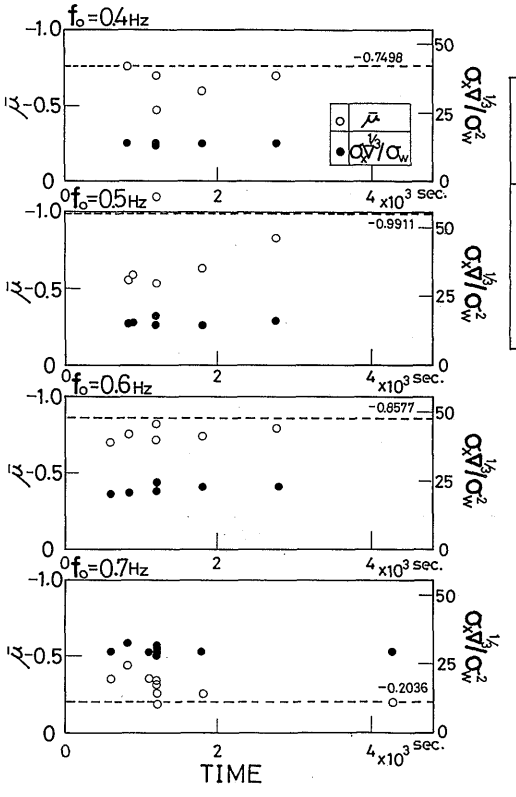

Fig. 15 Sample variances and skewnesses of surge motion as a time function

Table. 2 Comparisons with statistical values

Spectrum peak frequency (Hz)	sample statistical values		estimated statistical values	
	variance (cm^2) $\tilde{\sigma}_x^2$	skewness $\tilde{\mu}$	variance (cm^2) $\bar{\sigma}_x^2$	skewness $\bar{\mu}$
0.4	8.98	-0.703	8.63	-0.7498
0.5	11.80	-0.839	10.92	-0.9911
0.6	30.84	-0.7787	31.06	-0.8577
0.7	64.50	-0.1976	63.23	-0.2036

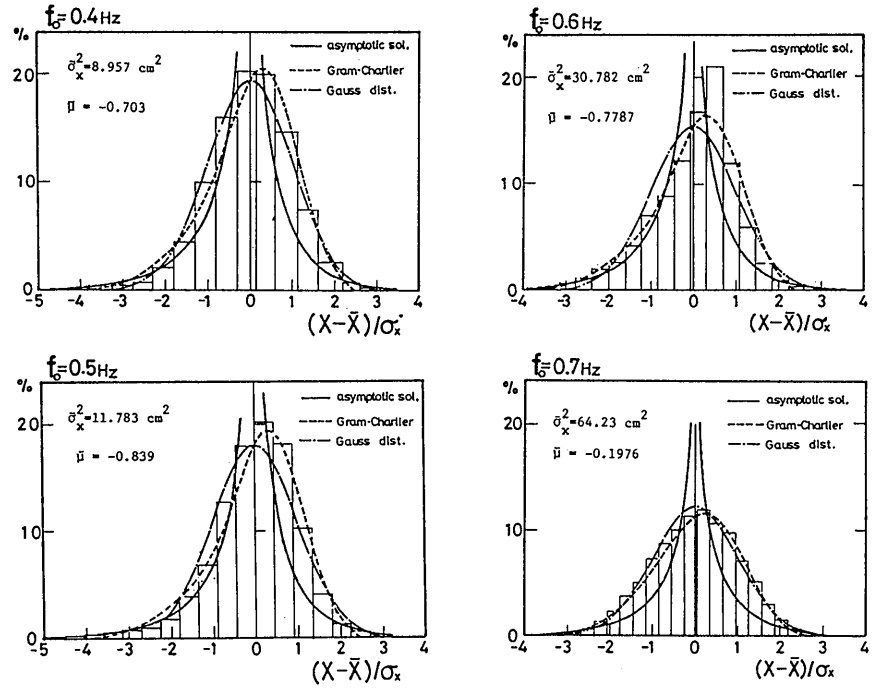

Fig. 16 Comparisons between observed histograms and estimated instantaneous probability distributions of surge motion

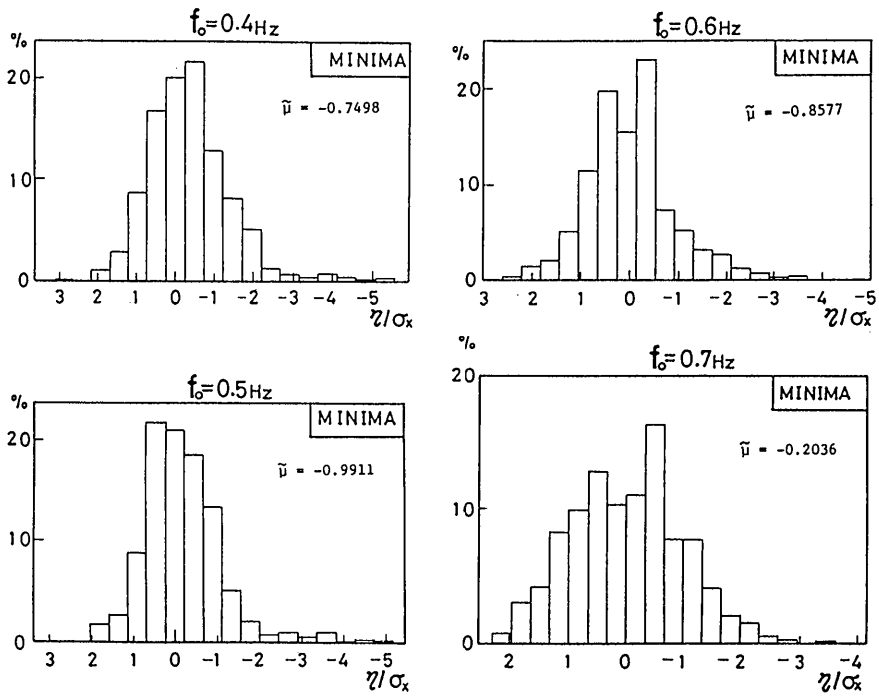

Fig. 17 Observed histograms of minima of surge motion

motions is given by matching between the both approximate solutions.

4.5 Investigation to Probability Distributions of Extremal Values and Extreme Value

If the co-ordinate system is taken as shown in Fig. 2, minima in extremal values are more important than maxima for the mooring design purpose. The probability distributions of minima are shown in Fig. 17 and that of the negative minima which are the most important in the estimation of the maximum mooring force are shown in Fig. 18. In Fig. 18 the solid line is the curve estimated from the asymptotic solution of exact instantaneous probability density function, and the broken line is that from the three term Gram-Charlier

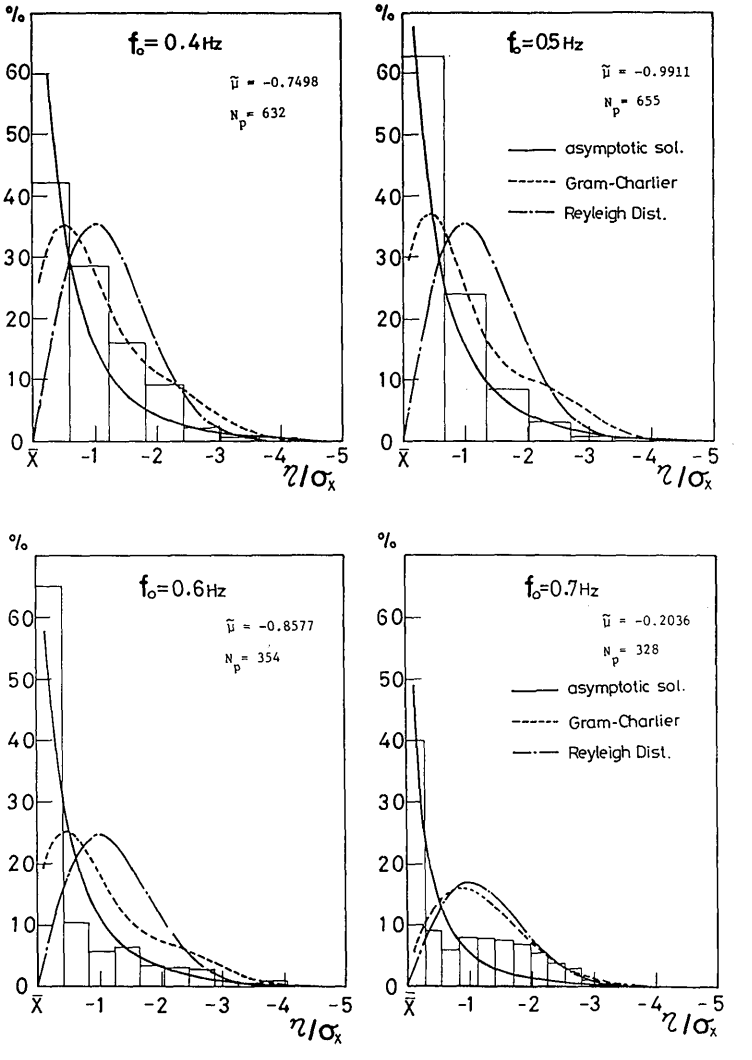

Fig. 18 Comparisons between observed histograms and estimated probability distributions of negative minima of surge motion

expansion and the dash-dot line is that from the Rayleigh distribution function. All curves in this figure are evaluated by using the estimated statistical values obtained from Table. 2. From these figures it is found that the probability distributions of minima depend remarkably on the skewness of the instantaneous probability distribution and the breadth of the distribution becomes wide with the increase of the absolute value of skewness and that the probability distributions of negative minima are fairly well represented by the curves estimated from the asymptotic solution of the exact instantaneous distribution. Fig. 19 shows the extreme values based on N_p observations of negative minima. The solid line shows the results obtained from the asymptotic solution, and the broken line shows those given the three term Gram-Charlier expansion, and the dash-dot line is the calculated value obtained by Longuet-Higgins[23]. The black circles indicate the experimental results obtained from each samples in total measuring data. The extreme values are normalized by the standard deviation of surge response, σ_x. From these figures it is found that the results from Longuet-Higgins's method significantly underestimate the extreme values of negative minima whereas those estimated from the asymptotic solution of the

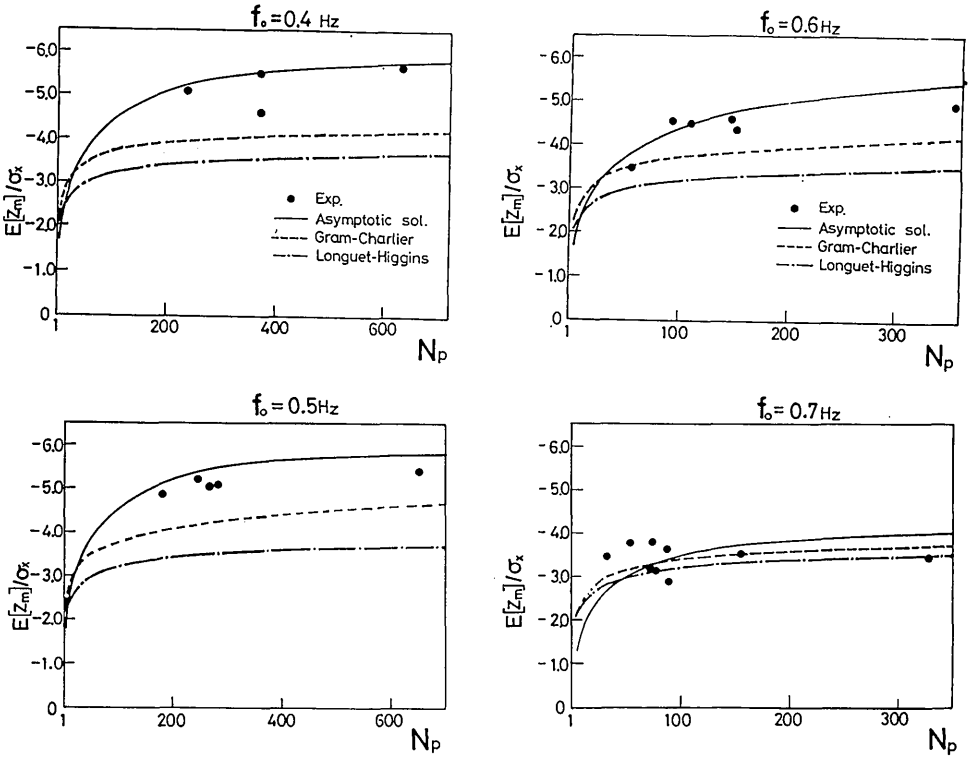

Fig. 19 Comparisons between observed extreme responses and estimated ones

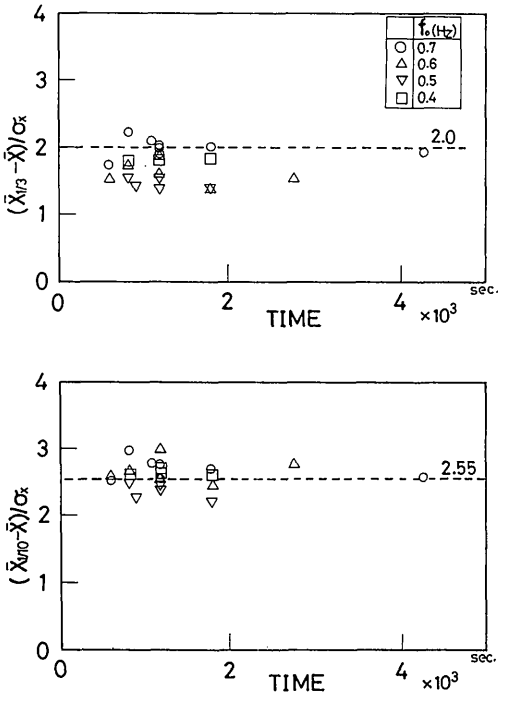

Fig. 20 Observed 1/n th highest expected amplitedes of surge motion

instantaneous probability density function show fairly good agreement with the experimental results.

Finally, Fig. 20 shows 1/n th highest expected amplitudes for the negative minima as a time function. In this figure the broken line is the result obtained from linear theory. From this figure it is found that 1/3 th highest expected amplitude is smaller than that from linear theory and in the case of 1/10 th highest amplitude the frequence exceeding the value of linear theory become high. In the estimation of these highest amplitudes Hineno's method[24] which extended Vinje's method to wide band random processes may be used.

5. CONCLUSIONS

The results of investigations on the statistical analysis of horizontal response of a moored floating structure are summarized as follows:

(1) If it is assumed that the horizontal response of a moored structure can be represented by two term Volterra series of incident wave, the instantaneous probability density function can be obtained exactly from both the eigenvalues and eigenfunctions of the Fredholm type integral equation of second kind with